



CineECG for visualization of changes in ventricular electrical activity during ischemia

I. van der Schaaf, MD^{a,*}, M. Kloosterman, MSc^a, A.P.M. Gorgels, MD PhD FESC^{b,c}, P. Loh, MD PhD^a, P.M. van Dam, PhD^{a,d}

^a Department of Cardiology, University Medical Center Utrecht, Heidelberglaan 100, 3584 CX Utrecht, the Netherlands

^b Department of Cardiology, Maastricht University Medical Center, P. Debyelaan 25, 6229 HX Maastricht, the Netherlands

^c Hartkliniek Maastricht, Victor de Stuersstraat 15, 6217 KP Maastricht, the Netherlands

^d ECG Excellence, Weijland 38, 2415 BC Nieuwerbrug, the Netherlands

ARTICLE INFO

Keywords:

CineECG

Ischemia

Electrocardiogram

ECG imaging

ABSTRACT

Background: CineECG offers a visual representation of the location and direction of the average ventricular electrical activity throughout a single cardiac cycle, based on the 12-lead ECG. Currently, CineECG has not been used to visualize ventricular activation patterns during ischemia.

Purpose: To determine the changes in ventricular activity during acute ischemia with the use of CineECG, and relating this to changes in the ECG.

Methods: Continuous ECG's during percutaneous coronary intervention with prolonged balloon inflation from the STAFF III database were analyzed with CineECG at baseline and every 10 s throughout the first 150 s of balloon inflation. The CineECG direction was determined for the initial QRS-complex, terminal QRS-complex, ST-segment and T-wave. Changes in the CineECG were quantified by calculating the Δ angle between the direction at baseline and the direction at every 10 s of inflation. Additionally, the root mean square amplitude (rmsA) of the ST-segment was computed.

Results: 94 patients were included. At start inflation, the median Δ angle was 14.7° [7.5–33.4], 21.8° [11.4–34.2], 20.6° [8.0–43.9], and 23.5° [11.8–48.0] for the initial QRS-complex, terminal QRS-complex, ST-segment and T-wave, respectively. Meanwhile, the median rmsA increased from 0.039 mV [0.027–0.058] at baseline to 0.045 mV [0.033–0.075] at start of inflation.

Conclusions: CineECG was able to detect immediate changes in ventricular electrical activity during induced ischemia, while changes in the ST-segment of the ECG were still subtle. Therefore, CineECG might support the early detection of acute ischemia, even before distinct ECG changes become visible.

Introduction

CineECG is a novel ECG technique which provides a quick and non-invasive way to estimate the location and direction of the average ventricular depolarization and repolarization. Using only the 12-lead ECG, this vectorcardiogram-based technique offers a quantitative visual representation of cardiac electrical activity, without taking the amplitude of the ECG-signal into account [1]. Previously, CineECG was proven useful in the identification of bundle branch blocks, substrate localization in Brugada syndrome, and has more recently been used to study atrial activation [2–5].

Until now, CineECG has not been utilized to investigate ventricular

electrical activity during cardiac ischemia. We hypothesize that CineECG is able to detect cardiac ischemia even when the ECG is inconclusive, since amplitude is not a part of the CineECG trajectory. Consequently, even small ST-deviations should be easily visualized. Therefore, the aim of this study was to establish the ability of CineECG to detect changes in ventricular electrical activity during cardiac ischemia.

Methods

Study population

The study population consisted of the patients from the STAFF III

* Corresponding author.

E-mail address: i.vanderschaaf-5@umcutrecht.nl (I. van der Schaaf).

<https://doi.org/10.1016/j.jelectrocard.2024.01.007>

Received 15 May 2023; Received in revised form 15 January 2024; Accepted 19 January 2024

Available online 27 January 2024

0022-0736/© 2024 The Authors. Published by Elsevier Inc. This is an open access article under the CC BY license (<http://creativecommons.org/licenses/by/4.0/>).

database [6,7]. This online, publicly available database consists of continuous ECG recordings during prolonged balloon inflation while percutaneous coronary intervention (PCI) was performed of one of the major coronary arteries (right coronary artery (RCA), left anterior descending (LAD), circumflex (Cx) branch, and left main coronary artery).

The following exclusion criteria were applied: 1.) Too much signal noise which prevented an accurate calculation of the CineECG, 2.) ECG's with ventricular arrhythmias. Patients with pre-existing ECG abnormalities were not excluded from this study.

CineECG

CineECG determines the location and the direction of the average ventricular activity during depolarization and repolarization. This provides a CineECG trajectory throughout the ventricles. The calculation of the CineECG trajectory is explained in detail in a previous paper [1].

CineECG requires only the input of a 12-lead ECG. If available, a personalized 3D model of the heart and torso can be used, as well as the specific electrode positions. As there were no patient models made during the STAFF III study, a standard heart model and electrode positions were used.

Data analysis

CineECG was used to analyze the baseline ECG and the ECG during PCI from start balloon inflation and at every 10 s until 150 s of balloon inflation. The baseline ECG was acquired during 5 min before catheter insertion at the catheterization laboratory. In case of two baseline recordings at the catheterization laboratory, the last baseline recording was used, assuming that this is the recording closest to the procedure. Only first balloon inflations were analyzed.

A median beat was created for every 10 s interval. The direction of the CineECG was determined for four segments: 1.) initial QRS-complex (first 25 ms of the QRS-complex), 2.) terminal QRS-complex (20 ms before the end of the QRS-complex - 30 ms after the end of the QRS-

complex), 3.) ST-segment (end of the QRS-complex - peak of the T-wave), and 4.) terminal T-wave (peak T-wave - end of the T-wave).

The changes in CineECG direction during balloon inflation relative to the direction at baseline were assessed by computing the Δangle . This was defined as the angle between the CineECG direction of the median beat at baseline and the CineECG direction of the median beat at every 10 s during balloon inflation (Fig. 1).

To evaluate ischemic changes in the 12-lead ECG, the root mean square amplitude of the ST-segment (rmsA) was determined by calculating the mean ST-amplitude (10–60 ms after the end of the QRS-complex). The ST-amplitude was calculated from the median beat, derived from the 12-leads, at baseline and for every 10 s of balloon inflation.

Two subgroup analyses were performed. One subgroup analysis was performed based on location of balloon inflation (RCA, LAD, Cx). The other subgroup analysis was based on amount of ST-deviation. For this analysis, the entire group was divided into two groups based on the maximum rmsA: 1.) A group with small changes in the ST-segment during balloon inflation (maximum rmsA <0.1 mV), and 2.) A group with greater changes in the ST-segment during balloon inflation (maximum rmsA \geq 0.1 mV). The maximum rmsA was defined as the highest value of the rmsA between 0 and 150 s of balloon inflation.

Appendix A includes an additional subgroup analysis on those patients where an ECG recording was available at the start of the procedure but prior to balloon inflation.

Data were analyzed using SPSS Statistics (version 27.0.0.0) and R Statistical Software (version 2022.07.2). The data was assessed for normality by using the Shapiro-Wilk's test. Normally distributed data were reported as mean \pm standard deviation and non-normally distributed data were reported as median and interquartile range.

Results

Baseline characteristics

Of the 104 patients from the STAFF III database, 10 patients were

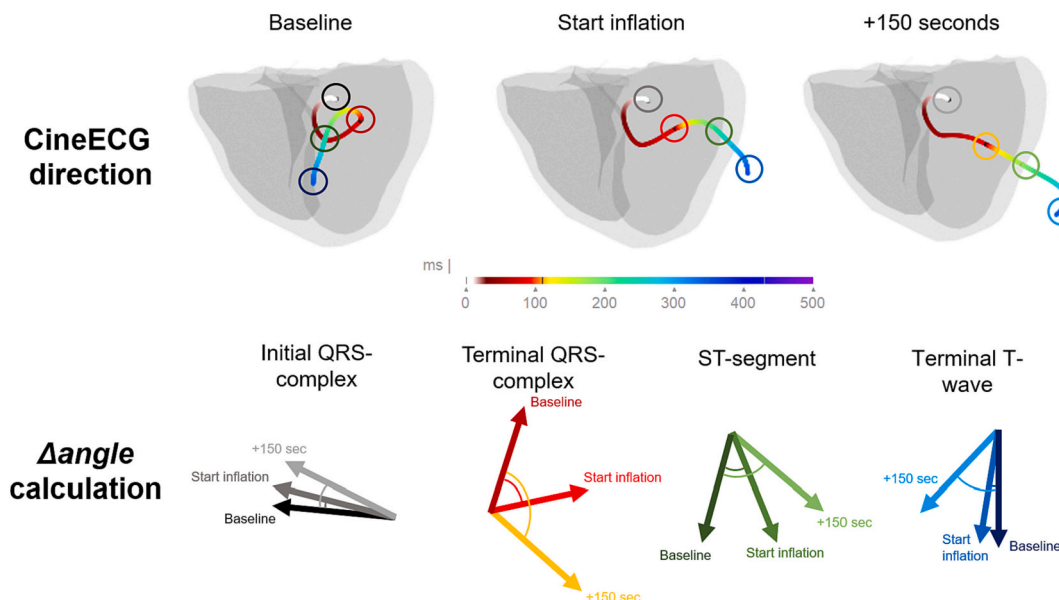


Fig. 1. Calculation of the Δangle . The upper row shows the CineECG trajectory at baseline, start inflation and at 150 s of inflation in one case example. The colour scale indicates that the CineECG is colored white at the earliest phase of depolarization, and blue at the latest phase of repolarization. At each time interval, the CineECG direction is determined for four segments; the initial QRS-complex (circled in black/grey), terminal QRS-complex (circled in red/orange), ST-segment (circled in green) and terminal T-wave (circled in blue). The lower row demonstrates the CineECG direction (represented by the colored arrows) at these three time intervals for the four segments. The colors of the arrows correspond with the circles in the upper row. The Δangle is calculated by determining the angle between the CineECG direction during balloon inflation and the CineECG direction at baseline. (For interpretation of the references to colour in this figure legend, the reader is referred to the web version of this article.)

excluded due to too much signal noise. In the remaining 94 patients (64.9% male, aged 61.4 ± 11.5 years), the median duration of balloon inflation was 296.0 [195.3–301.0] seconds. The RCA was the target vessel in 48.9% of the cases, the LAD in 29.8%, and the Cx in 20.2% of the cases. In one case the left main coronary artery was the target vessel. The precise location of the location of balloon inflation is stated in Table 1. Examples of the CineECG during balloon inflation of the RCA, LAD and Cx can be seen in Fig. 2.

Whole group analysis

The median Δ angle of the initial QRS-complex at the start of inflation was 14.7° [7.5–33.4], and reached its maximum at 90 s of balloon inflation (17.1° [6.3–34.4]). For the terminal QRS-complex, the median Δ angle at the start of inflation was 21.8° [11.4–34.2], and was greatest at 130 s of balloon inflation (41.0° [23.0–70.8]). The median Δ angle of the ST-segment increased from 20.6° [8.0–43.9] at start inflation to a maximum of 26.1° [13.1–56.0] at 140 s of balloon inflation. The terminal T-wave median Δ angle was 23.5° [11.8–48.0] at start of inflation and increased to a maximum of 26.3° [12.6–49.2] at 30 s of balloon inflation (Fig. 3A).

The median rmsA increased from 0.039 mV [0.027–0.058] at baseline to 0.045 mV [0.033–0.075] at start of inflation. The maximum rmsA was 0.084 mV [0.050–0.147] at 150 s of balloon inflation (Fig. 3B).

Subgroup analysis based on amount of ST-deviation

In the first group with a maximum rmsA <0.1 mV ($n = 46$), the median Δ angles at the start of balloon inflation were 13.1° [7.4–26.2], 23.4° [11.6–32.0], 19.2° [7.9–38.0], and 19.6° [11.7–39.2] for the initial QRS-complex, terminal QRS-complex, ST-segment and terminal T-wave, respectively (Fig. 3C). In the second group with a maximum rmsA ≥ 0.1 mV ($n = 45$), the initial median Δ angles were 18.0° [8.7–35.3], 21.4° [10.3–35.0], 22.9° [8.0–62.8], and 35.7° [12.1–66.8], respectively (Fig. 3D). In the first group, no great changes in Δ angle were observed during balloon inflation for either of the four segments. In the second group, most changes were observed in the Δ angle for the terminal QRS-complex, this increased to a maximum of 62.6° [37.7–108.2] at 140 s of balloon inflation. The Δ angle of the other three segments did not change much during balloon inflation.

Table 1

Baseline characteristics. Data is presented as n (%), mean \pm standard deviation or median [Q1 – Q3]. LAD = left anterior descending, RCA = right coronary artery, Cx = Circumflex.

Baseline characteristics	
Male (n)	61 (64.9%)
Age (years)	61.4 ± 11.5
Duration of balloon inflation (s)	296.0 [195.3–301.0]
LAD occlusions (n)	28 (29.8%)
- Proximal LAD	19 (20.2%)
- Proximal – mid LAD	2 (2.1%)
- LAD diagonal	1 (1.1%)
- Mid LAD	6 (6.4%)
RCA occlusions (n)	46 (48.9%)
- Proximal RCA	18 (19.1%)
- Proximal – mid RCA	2 (2.1%)
- Mid RCA	14 (14.9%)
- Distal RCA	12 (12.8%)
Cx occlusions (n)	19 (20.2%)
- Proximal Cx	9 (9.6%)
- Mid Cx	4 (4.3%)
- Distal Cx	6 (6.4%)
Left main occlusions (n)	1 (1.1%)

Subgroup analysis based on location of balloon inflation

Right coronary artery

The initial median Δ angle for the initial QRS-complex was 11.1° [6.8–15.6] and reached its maximum at 40 s of balloon inflation (14.7° [7.7–26.7]). For the terminal QRS-complex, the median Δ angle at the start of inflation was 25.2° [12.6–36.6] and was greatest at 130 s of balloon inflation (42.0° [25.5–54.9]). The median Δ angle of the ST-segment increased from 20.5° [8.2–36.5] at the start of inflation to 24.3° [13.7–45.5] at 40 s of balloon inflation. The terminal T-wave median Δ angle was 20.5° [11.7–40.0] at baseline and increased to 26.1° [11.6–38.7] at 30 s of balloon inflation (Fig. 3E).

The median rmsA was 0.039 mV [0.027–0.056] at baseline, and 0.038 mV [0.029–0.055] at start inflation. The highest median rmsA for the ST-segment was 0.07 mV [0.041–0.093] at 150 s of balloon inflation (Fig. 3H).

Left anterior descending

The median Δ angle of the initial QRS-complex the start of balloon inflation was 29.1° [14.9–42.8], and reached its maximum at 10 s of balloon inflation (32.9° [13.2–56.0]). For the terminal QRS-complex, the median Δ angle at the start of inflation was 21.4° [13.4–35.9], and was greatest at 140 s of balloon inflation (89.5° [40.4–138.5]). The median Δ angle of the ST-segment increased from 14.3° [7.8–50.0] to 22.9° [10.1–49.0] at 150 s of balloon inflation. The terminal T-wave median Δ angle was highest at start inflation (31.9° [10.1–44.4]) (Fig. 3F).

The median rmsA was 0.035 mV [0.027–0.056] at baseline and increased to 0.051 mV [0.036–0.095] at start of balloon inflation. The maximum median rmsA was 0.205 mV [0.119–0.280] at 130 s of balloon inflation (Fig. 3H).

Circumflex

The initial median Δ angle at the start of balloon inflation was 13.4° [6.3–41.2], and reached its maximum at 50 s of balloon inflation (25.0° [16.7–36.4]). For the terminal QRS-complex, the median Δ angle at the start of inflation was 16.5° [7.2–26.9], and was greatest at 150 s of balloon inflation (26.9° [16.2–41.0]). The median Δ angle of the ST-segment increased from 28.6° [7.6–71.1] to 72.9° [29.8–95.4] at 150 s of balloon inflation. The terminal T-wave median Δ angle was maximally 47.6° [19.7–62.3] at start inflation (Fig. 3G).

The median rmsA was 0.039 mV [0.022–0.062] at baseline, and 0.065 mV [0.041–0.100] at start of balloon inflation. The maximum rmsA was 0.085 mV [0.050–0.112] at 150 s of balloon inflation (Fig. 3H).

Discussion

This study was able to show the dynamics in the ventricular electrical activity during ischemia. With the use of CineECG, early changes in the activation pattern were observed. Interestingly, while changes in the CineECG direction were seen directly at start of balloon inflation, the ST-segment in the 12-lead ECG was only minimally changed at this point (increase in median rmsA of 0.006 mV). This is an important finding, considering that deviation of the ST-segment is highly important in diagnosing ischemia with the use of an ECG [8,9]. Presumably, this finding can be explained by the amplitudes in the 12-lead ECG not being taken into account in the calculation of the CineECG trajectory. As a result, CineECG presents smaller ST-deviations in the ECG in a similar manner as greater ST-deviations. Thus, the CineECG is already highly affected while the amount of ischemia is still minimal. Possibly, merely the insertion of the catheter into the (partly occluded) coronary arteries caused the immediate changes in the CineECG trajectory at the start of balloon inflation.

The susceptibility of CineECG to detect subtle changes in the ECG is furthermore underlined by the observation that even in the subgroup

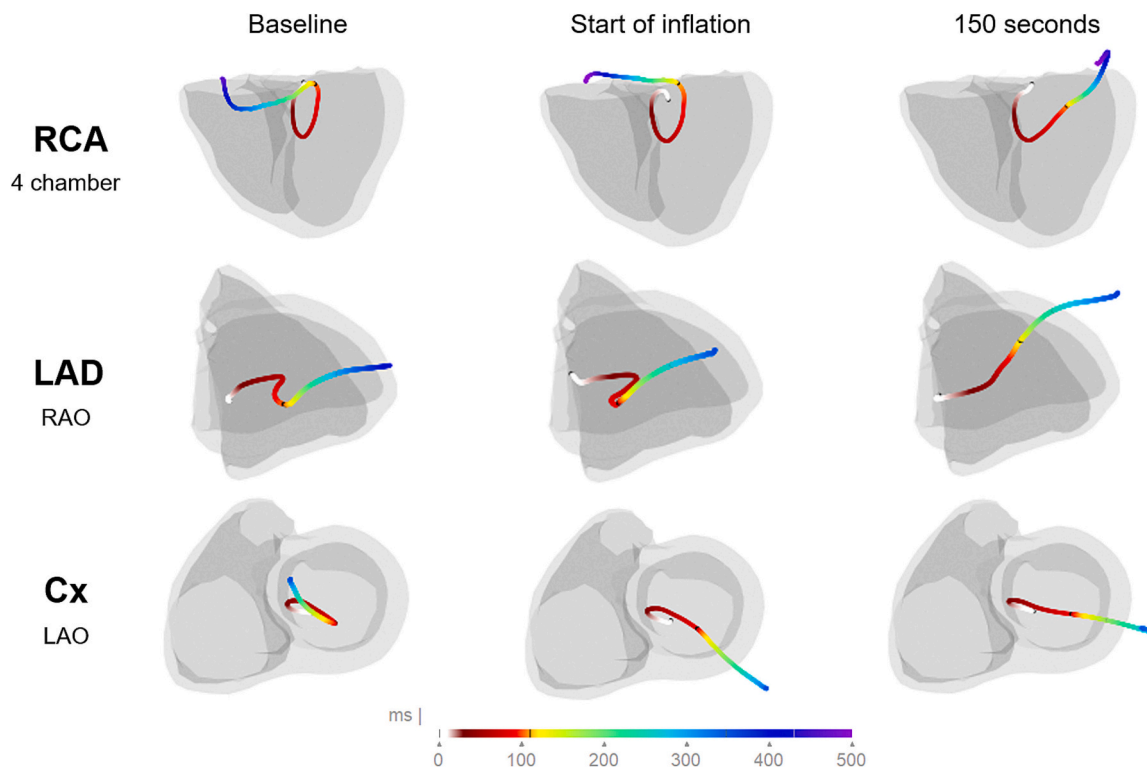


Fig. 2. Examples of the CineECG trajectory for three different locations of balloon inflation. The CineECG during right coronary artery (RCA) occlusion from a 4 chamber view is shown in the upper row. The overall CineECG direction moves to the left basal area of the heart during balloon inflation. The CineECG during left anterior descending (LAD) occlusion from a right anterior oblique (RAO) view is seen in the middle row. The CineECG trajectory becomes elongated and is directed towards the anterior part of the heart during balloon inflation. The CineECG during a circumflex (Cx) occlusion from a left anterior oblique (LAO) view is seen in the lower row. The overall CineECG direction starts to move towards the inferolateral part of the heart during balloon inflation. The CineECG is shown at baseline, at the start of balloon inflation, and at 150 s of balloon inflation. Below, a colour scale is shown, indicating the CineECG is colored white at the earliest phase of depolarization, and blue at the latest phase of repolarization. (For interpretation of the references to colour in this figure legend, the reader is referred to the web version of this article.)

without great ST-changes during balloon inflation, the Δ angles at the start of balloon inflation were rather substantial. Apart from slight deviations of the ST-segment, the CineECG could have been affected by other changes in the ECG due to the induced ischemia, such as changes in the QRS-complex or T-wave. These ECG characteristics were not part of this study. Still, this is a promising finding, and could mean that the CineECG might be affected in non-ST-elevation acute coronary syndrome (NSTEMI-ACS) patients, therefore possibly providing a way to improve diagnosis in this patient population.

Furthermore, the results of this study showed that the CineECG trajectory was affected by occlusions of all three major coronary arteries. Although the observed changes in Δ angle over time were similar in LAD and RCA occlusions – showing the greatest changes occurring in the terminal QRS-segment during balloon inflation – a different pattern was seen in Cx occlusions. In these type of occlusions, the greatest changes were observed in the ST-segment of the CineECG trajectory. This different pattern might occur because the Cx supplies the blood to the posterolateral part of the heart, which is activated latest during the cardiac cycle [10–12]. Therefore, the terminal QRS-complex in the CineECG trajectory might not be very affected in Cx occlusions.

In **Appendix A**, additional analysis was performed in the patients where an ECG recording was available during the PCI procedure but prior to the start of balloon inflation. Here, a trend was observed that the Δ angles started to increase before the start of balloon inflation, although no significant changes were observed. These results could indicate that CineECG is extremely sensitive to ischemic changes, as in this time period the catheter must have been inserted or repositioned within the coronary artery and contrast could have been injected. These could have had a small ischemic effect, and may therefore have contributed to the

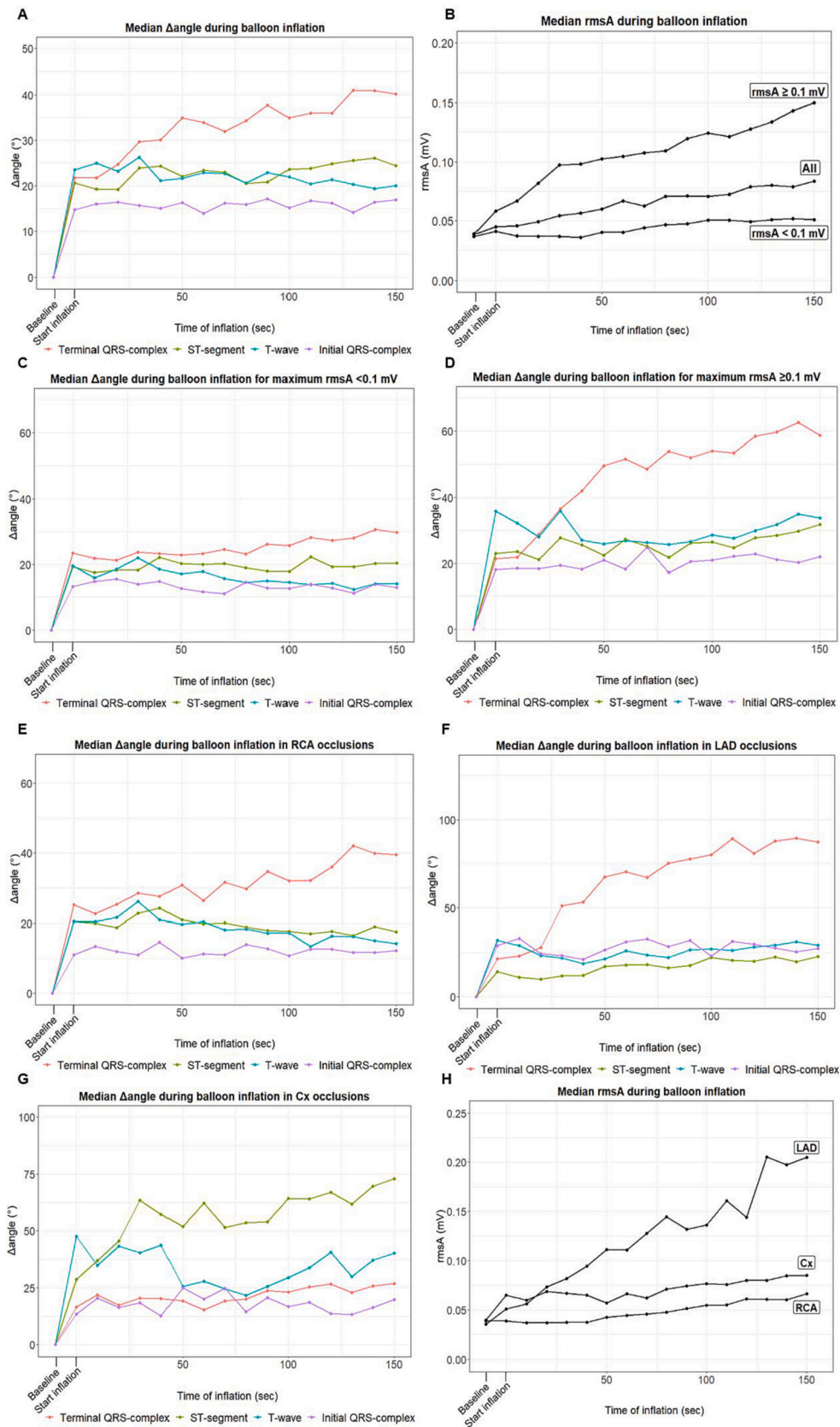
observed Δ angles prior to balloon inflation. However, this hypothesis can only be tested if the circumstances of the pre-inflation ECG's would have been annotated. An alternative explanation for the observed Δ angles before balloon inflation is that there might always be a slight difference between two different CineECG trajectories within the same subject. Thus, a Δ angle may always be present to some extent, which is unrelated to ischemia.

Limitations

A limitation of this study is that there was no information available on the cardiac history or possible other lesions in the coronary arteries. Exposure to (prior) ischemia could have led to the formation of collaterals and/or scar tissue. The possible influences that this could have had on the CineECG trajectory are unknown. Thus, these results should be interpreted while taking this into consideration.

Moreover, a standardized heart torso model was used with standard electrode positions. Patient specific models and electrode positions could have made the results of this study more reliable to interpret. However, in a previous study, CineECG was shown to be robust to varying electrode positions as well as heart torso model errors [1].

This study only looked at the ECG recordings at baseline and during the first 150 s of balloon inflation, while the median time of balloon inflation was close to 300 s. Therefore, a lot of the available data was not analyzed. This was done because at 150 s the balloon inflation had ended in 10% of the patients. We hypothesized that patients with longer durations (>150 s) of balloon inflation were less likely to have ECG dynamics, possibly due to prior ischemic events. This could have led to bias while analyzing the data. Hence, the ECG recordings after 150 s of



(caption on next page)

Fig. 3. A) The median $\Delta angle$ during balloon inflation. B) The median root mean square amplitude of the ST-segment (rmsA) at baseline and during balloon inflation for the whole group (“All”) and the subgroups of patients with a maximum rmsA <0.1 mV and ≥ 0.1 mV. C) The median $\Delta angle$ during balloon inflation for the patients with a maximum rmsA <0.1 mV. D) The median $\Delta angle$ during balloon inflation for the patients with a maximum rmsA ≥ 0.1 mV. E) The median $\Delta angle$ during balloon inflation of the right coronary artery (RCA). F) The median $\Delta angle$ during balloon inflation of the left anterior descending (LAD). G) The median $\Delta angle$ during balloon inflation of the circumflex (Cx). H) The median rmsA at baseline and during balloon inflation for each subgroup based on location of balloon inflation. Purple = initial QRS-complex, red = terminal QRS-complex, green = ST-segment, blue = T-wave. (For interpretation of the references to colour in this figure legend, the reader is referred to the web version of this article.)

balloon inflation were not included in this study. Even so, by excluding the ECG’s made after 150 s of balloon inflation, important information could have been missed in this study. Moreover, the recordings between start of the procedure and before balloon inflation were not available in many cases, and it is not clear what happened during these pre-inflation ECG’s (such as moment of catheter insertion, possible contrast injection or movement of the catheter). The results from this analysis (**Appendix A**) are therefore difficult to interpret.

Finally, the method that was used in this study required a baseline ECG, which is not always available in clinical practice. The calculation of the $\Delta angle$ will not be possible in many clinical cases. However, with this study, we have been able to establish the susceptibility of CineECG for changes in electrical activity during ischemia. Furthermore, it underlines the importance of a reference ECG in the interpretation of the 12-lead ECG of patients suspected of myocardial ischemia.

Future directions

Future research should focus on defining the CineECG characteristics during ischemia in a well-defined population which includes information on medical history and coronary anatomy. Moreover, future studies should investigate the added value of CineECG in NSTEMI-ACS, as this is the population where the 12-lead ECG cannot always provide an early diagnosis. Particular focus should lie on the patient population where no reference ECG is available. CineECG might then be especially helpful in a pre-hospital setting in patients with non-typical complaints, to direct triage decisions and to refer the patient to an interventional hospital if appropriate.

Conclusions

CineECG was able to detect early changes in ventricular de- and repolarization due to obstructions in all three coronary arteries even before great changes in the ST-segment had occurred, as determined by the rmsA. CineECG is therefore a promising new tool in the detection of acute ischemia in the absence of clear ST-deviations.

Funding

This work was supported by Eurostars (project ID 115220 | CineECGPlus) in collaboration with ECG Excellence (NL), Epique (GE) and IRCCS Policlinico San Donato Milanese (IT).

CRediT authorship contribution statement

I. van der Schaaf: Writing – original draft, Visualization, Methodology, Investigation, Formal analysis, Conceptualization. **M. Kloosterman:** Writing – original draft, Conceptualization. **A.P.M. Gorgels:** Writing – review & editing, Supervision, Conceptualization. **P. Loh:** Writing – review & editing, Supervision, Conceptualization. **P.M. van**

Dam: Writing – review & editing, Supervision, Software, Conceptualization.

Declaration of competing interest

Peter van Dam is owner of ECG Excellence BV / Peacs BV.

Appendix A. Supplementary data

Supplementary data to this article can be found online at <https://doi.org/10.1016/j.jelectrocard.2024.01.007>.

References

- [1] Boonstra MJ, Brooks DH, Loh P, van Dam PM. CineECG: a novel method to image the average activation sequence in the heart from the 12-lead ECG. *Comput Biol Med* 2022;141:105128. <https://doi.org/10.1016/j.combiomed.2021.105128>.
- [2] Boonstra MJ, Hilderink BN, Locati ET, Asselbergs FW, Loh P, van Dam PM. Novel CineECG enables anatomical 3D localization and classification of bundle branch blocks. *EP Europace* 2021;23(Supplement 1):i80–7. <https://doi.org/10.1093/europace/eaab396>.
- [3] van der Schaaf I, Kloosterman M, Boonstra MJ, van Dam PM, Gorgels APM. CineECG illustrating the ventricular activation sequence in progressive AV-junctional conduction block. *J Electrocardiol* 2023;78:1–4. <https://doi.org/10.1016/j.jelectrocard.2023.01.004>.
- [4] van Dam PM, Locati ET, Ciccone G, Borrelli V, Heilbron F, Santinelli V, et al. Novel CineECG derived from standard 12-Lead ECG enables right ventricle outflow tract localization of electrical substrate in patients with Brugada syndrome. *Circ Arrhythm Electrophysiol* 2020;13(9):e008524. <https://doi.org/10.1161/CIRCEP.120.008524>.
- [5] Locati ET, Pappone C, Heilbron F, van Dam PM. CineECG provides a novel anatomical view on the normal atrial P-wave. *Eur Heart J Digit Health* 2022;3(2):169–80. <https://doi.org/10.1093/ehjdh/ztac007>.
- [6] Goldberger AL, Amaral LA, Glass L, Hausdorff JM, Ivanov PC, Mark RG, et al. PhysioBank, PhysioToolkit, and PhysioNet: components of a new research resource for complex physiologic signals. *Circulation* 2000;101(23):E215–20. <https://doi.org/10.1161/01.CIR.101.23.e215>.
- [7] Martínez JP, Pahlm O, Ringborn M, Warren S, Laguna P, Sörnmo L. The STAFF III database: ECGs recorded during acutely induced myocardial ischemia. *Comput Cardiol* 2017;44:266–133.
- [8] Collet JP, Thiele H, Barbato E, Barthélémy O, Bauersachs J, Bhatt DL, et al. 2020 ESC guidelines for the management of acute coronary syndromes in patients presenting without persistent ST-segment elevation. *Eur Heart J* 2021;42(14):1289–367. <https://doi.org/10.1093/eurheartj/ehaa575>.
- [9] Ibanez B, James S, Agewall S, Antunes MJ, Bucciarelli-Ducci C, Bueno H, et al. 2017 ESC guidelines for the management of acute myocardial infarction in patients presenting with ST-segment elevation. *Eur Heart J* 2018;39(2):119–77. <https://doi.org/10.1093/eurheartj/ehx393>.
- [10] Ortiz-Pérez JT, Rodríguez J, Meyers SN, Lee DC, Davidson C, Wu E. Correspondence between the 17-segment model and coronary arterial anatomy using contrast-enhanced cardiac magnetic resonance imaging. *JACC Cardiovasc Imaging* 2008;1(3):282–93. <https://doi.org/10.1016/j.jcmg.2008.01.014>.
- [11] Donato P, Coelho P, Santos C, Bernardes A, Caseiro-Alves F. Correspondence between left ventricular 17 myocardial segments and coronary anatomy obtained by multi-detector computed tomography: an ex vivo contribution. *Surg Radiol Anat* 2012;34(9):805–10. <https://doi.org/10.1007/s00276-012-0976-1>.
- [12] Durrer D, Van Dam RT, Freud GE, Janse MJ, Meijler FL, Arzbaecher RC. Total excitation of the isolated human heart. *Circulation* 1970;41(6):899–912. <https://doi.org/10.1161/01.cir.41.6.899>.